Petrography and geochemistry of the Ab-e-Haji Formation in central Iran: implications for provenance and tectonic setting in the southern part of the Tabas block

Mahdi Shadan[1, *] and Mahboubeh Hosseini-Barzi[2, **]

[1] Corporation of Engineering, Zamin Rizkavan, No. 6 Saeedi Exp., Azadi Sq., Tehran, Iran.
[2] Department of Geology, Faculty of Earth Sciences, Shahid Beheshti University, Tehran, Iran.
**shadangeo@gmail.com ** m_hosseini@sbu.ac.ir*

ABSTRACT

Sandstone petrography and shale geochemistry from the lower Jurassic Ab-e-Haji Formation, in the southern part of Tabas block, were used to constrain provenance, tectonic setting and weathering conditions. The sandstones consist mainly of quartz and sedimentary and low grade metamorphic lithic fragments and therefore, show quartzolithic nature (Qm_{38}-F_2-Lt_{60}, $Qt5_8$-F_2-L_{40}). However, modal analysis as well as highly labile lithics in Ab-e-Haji sandstones point to short transport of sandstone components from a recycled source of a fold thrust belt to its nearby foreland basin. Discrimination diagrams based on major and trace elemen content point to a role of recycled sources for the deposition of Ab-e-Haji Formation, which at the upper part of the section were probably mixed with a minor felsic source. Negative Eu anomalies, similar to those displayed by Post-Archean Australian Shale (PAAS), along with depleted Ca, Na, Cs, Ba and Rb, and low K_2O/Al_2O_3 ratios in studied shales, suggest low abundance of feldspar in the source terrane. Depletion of transition metals (Cu, Sc, Ni, Cr, and V) can be explained by derivation from a more silicic and fractionated source than the PAAS. Moreover, the geochemical results from La–Th–Sc diagram as well as La/Sc, Th/Cr, and Th/Sc ratios of Ab-e-Haji sediments are within the range of fine-grained sediments derived from silicic sources. The chondrite-normalized rare earth elements (REE) patterns of samples are similar to those of PAAS, with light REE enrichment, a negative Eu anomaly, and almost flat heavy REE pattern, similar to those of a source rock with felsic and (meta) sedimentary components. Most probably, displacement of intrabasinal faults, such as the active Kuh-Banan basement fault, and exposure of supracrustal successions (fold thrust belt) provided a mixed source area that supplied the sediments for the Ab-e-Haji foreland basin. This tectonic activity could have been related to the Eo-Cimmerain orogeny in central Iran during the Late Triassic to Jurassic. Furthermore, the point counting data from Ab-e-Haji sandstones imply a semi humid climatic condition, which is supported by the CIA (chemical index of alteration) values for the shales of this formation, which indicate moderate to intense weathering of the parent rocks in the source area.

Key words: petrography, geochemistry, provenance, Ab-e-Haji Formation, Tabas block, central Iran.

RESUMEN

Estudios petrográficos de areniscas y geoquímica de lutitas de la Formación Ab-e-Haji del Jurásico Inferior, perteneciente a la parte sur del bloque de Tabas en Irán central, se emplearon para constreñir la proveniencia, ambiente tectónico y condiciones de intemperismo. Las areniscas están constituidas

principalmente por cuarzo y fragmentos líticos sedimentarios y metamórficos de bajo grado y, por lo tanto son de naturaleza cuarzolítica (Qm_{38}-F_2-Lt_{60}, Qt_{58}-F_2-L_{40}). Sin embargo, el análisis modal, con presencia de líticos muy inestables, de la Formación Ab-e-Haji indica poco transporte de los componentes de las areniscas desde un cinturón de pliegues y cabalgaduras a la cuenca de antepaís. Diagramas de discriminación basados en el contenido de elementos mayores y traza indican la participación de fuentes recicladas en el depósito de la Formación Ab-e-Haji, las cuales, en la parte superior de la sección, fueron probablemente mezcladas con una fuente félsica menor. Anomalías negativas de Eu, similares a las que presentan la Lutita Australiana Post-Arqueana (PAAS, por sus siglas en inglés), así como el empobrecimiento en Ca, Na, Cs, Ba y Rb y una baja relación de K_2O/Al_2O_3 en las lutitas estudiadas, sugiere una baja abundancia de feldespato en la fuente. El empobrecimiento en los metales de transición (Cu, Sc, Ni, Cr y V) puede explicarse por la derivación de una fuente más silícica y fraccionada que la PAAS. Además, de acuerdo con el diagrama de La–Th–Sc y las relaciones La/Sc, Th/Cr y Th/Sc, los sedimentos de la Formación Ab-e-Haji están dentro del rango de sedimentos finos derivados de fuentes silícicas. Los patrones de elementos de las tierras raras (REE) normalizados a condrita son similares a los de la PAAS, con enriquecimiento de tierras raras ligeras (LREE), anomalía negativa de Eu y un patrón casi plano de las tierras raras pesadas (HREE), características similares a las de rocas fuente con componentes félsicos y (meta)sedimentarios. Se interpreta que el desplazamiento de fallas intracuenca, como la falla de basamento activa Kuh-Banan, y la exposición de sucesiones supracrustales (cinturón de pliegues y cabalgaduras), constituyeron un área fuente mixta que aportó sedimentos a la cuenca de antepaís Ab-e-Haji. Esta actividad tectónica pudo estar relacionada con la orogenia Eo-Cimmeriana en Irán central durante el Tirásico tardío al Jurásico. Por otra parte, los datos del conteo de puntos en areniscas de la Formación Ab-e-Haji apunta a condiciones climática semihúmedas, lo cual es respaldado por los valores del índice químico de alteración de las lutitas de esta formación, los cuales indican intemperismo moderado a intenso de las rocas parentales en el área fuente.

Palabras clave: petrografía, geoquímica, procedencia, Formación Ab-e-Haji, bloque Tabas, Irán central.

INTRODUCTION

Petrography and geochemical compositions of siliciclastic rocks provide important information on the provenance as well as tectonic setting (*e.g.,* van de Kamp and Leake, 1995; Cingolani *et al.*, 2003, Armstrong-Altrin and Verma 2005, Nagarajan *et al.,* 2007, Jafarzadeh and Hosseini-Barzi 2008). Provenance studies on arenites are generally performed following a classical approach based on petrographic modal analysis (*e.g.,* Dickinson, 1970; Ingersoll 1978; Pettijohn *et al.*, 1987; Johnson, 1993; Garzanti *et al.*, 1996). However, numerous criteria for the chemical discrimination of provenance type have been published, which are a useful complement to the constraints from petrographic analysis (*e.g.*, Cullers *et al.*, 1988; McLennan *et al.*, 1993; Cullers, 2000,). In geochemical provenance studies, fine grained sedimentary rocks like shales are considered to be the most useful because of their thorough homogenization before deposition, post-depositional impermeability and higher abundance of trace elements (Taylor and McLennan, 1985; Condie, 1993; McLennan *et al.*, 2000; Bracciali *et al.*, 2007). It is well established that some relatively immobile elements such as rare earth elements (REE), Sc, Th, Zr, and Hf, show very low concentrations in natural waters and are transferred nearly quantitatively throughout the sedimentary process from parent rocks to clastic sediments (Taylor and McLennan, 1985; Condie, 1991). Also, some major elements such as alkali and alkali earth elements, which are water mobile elements and very sensitive to climatic change, can be used as a proxy of paleoclimate evolution (Nesbitt and Young, 1984; Wei *et al.*, 2004).

Although central Iran represents an important tectonic province in the Middle East, only a few provenance studies for this region have been conducted. During lower Cambrian, central Iran experienced tensional tectonics resulting in the development of small pull-apart basins along with exposure of felsic rocks of the Pan-African basement (Etemad-Saeed *et al.*, 2011). Provenance studies of Devonian (Saeedi and Hosseini-Barzi, 2010) and Permian (Shadan and Hosseini-Barzi, 2009) deposits in central Iran implied the existence of a dominant cratonic and recycled source. Moreover, Balini *et al.* (2009) denoted a magmatic arc provenance and deposition in an arc-related setting for Triassic siliciclastic successions of central Iran. Therefore, the present study might clarify some consequences of the Eo-Cimmerian (Late Triassic) orogeny in this region.

The main purpose of this paper is to evaluate the composition and petrography of sandstones, and the geochemistry (major, trace, and rare earth elements) of fine-grained sediments of the Ab-e-Haji Formation (an economic important coal-bearing deposit in central Iran zone) in order to provide information on the provenance of detrital material and paleoweathering, and to constrain the tectonic setting of the southern part of the Tabas block in central Iran.

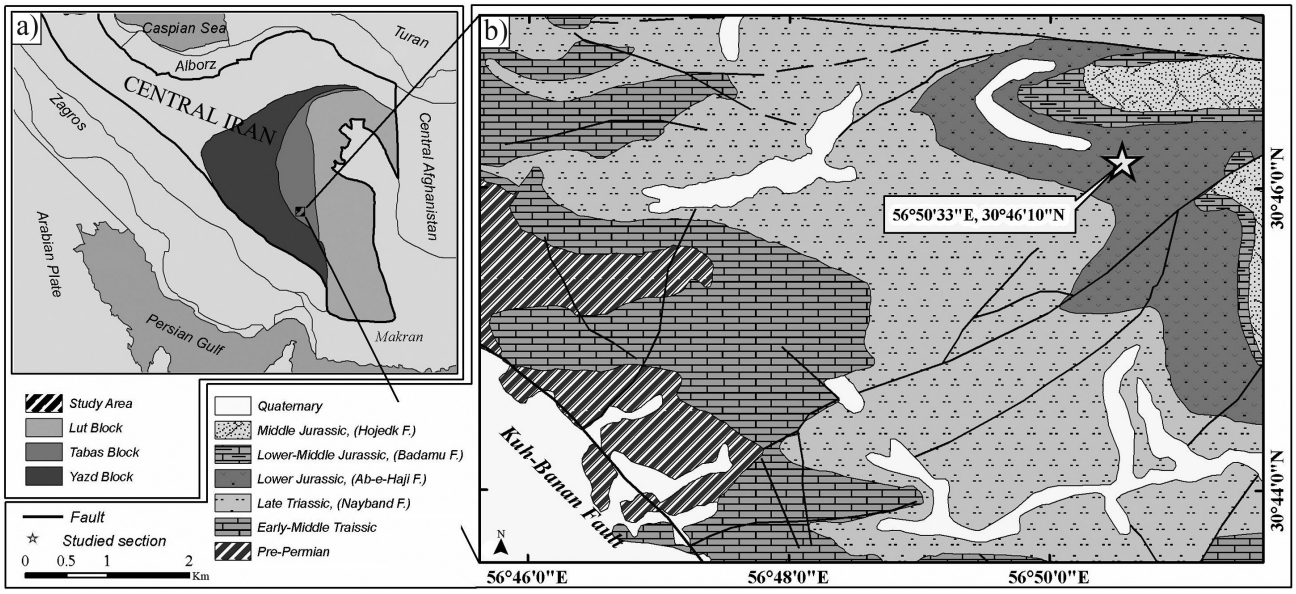

Figure 1. a: Tectonic scheme of Iran showing the main tectonic subdivisions (modified from Geological Survey of Iran, 1989). b: Simplified geological map of the study area in the southern part of the Tabas block; the location of the studied Dar-e-Bidkhoon section is indicated by the star.

GEOLOGICAL SETTING

Central Iran occupies a key position for unraveling the post-Eo-Cimmerian Mesozoic history. As a segment of the Cimmerian microplates, central Iran, including the Tabas block (Figure 1), was separated from Gondwana (Arabian plate) during the Late Permian and collided with Eurasia (Turan plate) in the Late Triassic (*e.g.*, Berberian and King, 1981; Alavi *et al.*, 1997; Stampfli and Borel, 2002).

Eo-Cimmerian tectonics and related syn-sedimentary fault tectonics caused the formation of troughs in different parts of Iran, including the southern part of the Tabas block (Davoudzadeh *et al.*, 1981; Fursich *et al.*, 2005). In the later region, the onset of Eo-Cimmerian deformation caused a dramatic change from Middle Triassic platform carbonates (Shotori Formation) to dominantly siliciclastic sediments of the Shemshak group. Therefore, study of the very thick and well-exposed Upper Triassic–Middle Jurassic sequences of the Shemshak group (Nayband, Ab-e-Haji, Badamu, and Hojedk formations) is crucial for the understanding of the Mesozoic evolution of the Iranian plate.

At the Triassic–Jurassic boundary, the formation of completely marine sediments of the Late Triassic Nayband Formation (the first member of Shemshak group) was followed by the Lower Jurassic Ab-e-Haji Formation (Figure 2), which was deposited in a fluvial-coastal plain environment (Wilmsen *et al.*, 2009). The Ab-e-Haji Formation unconformably overlies the Nayband Formation and underlies shallow marine carbonates of the Badamu Formation. In this work, to study the Ab-e-Haji Formation (Figure 1), the Dar-e-Bidkhoon section (Figure 2), located in the east of the Kuh-Bannan basement fault in the southern part of the Tabas block, was sampled. In this section, Ab-e-Haji Formation consists of greenish shale, siltstone, and sandstone with few coal seams.

METHODS

One hundred and twenty fresh sandstone, compositionally immature litharenite, and pure to fossiliferous shale samples were collected from the Dar-e-Bidkhoon section of the Ab-e-Haji Formation. Forty-three polished thin sections from sandstones were petroghraphically studied. Point counting of more than 300 points per thin section was performed on twenty sandstone samples. In order to reduce the effect of the grain size on the point-counting results, well-sorted (least standard deviation in grain size), medium size sandstone samples were chosen for quantitative compositional analysis (Pirrie, 1991; Lee and Sheen, 1998). Moreover, using the Gazzi–Dickinson point-counting method (Gazzi, 1966; Dickinson, 1970), we minimized this effect on our modal analysis results (Ingersoll *et al.*, 1984). However, lithic fragment identification followed the objective criteria of Dorsey (1988), and Garzanti and Vezzoli (2003). Feldspar and lithic fragments, regardless of degree of alteration or replacement, were counted as the original grain types if these were positively identified on the basis of remnant textures.

Since fine-grained siliciclastic rocks are more useful in geochemical studies than the coarser ones (*e.g.*, McLennan *et al.*, 2000; Bracciali *et al.*, 2007), fourteen samples of shale were selected to cover the entire section and analyzed for major and trace elements, including the rare earth elements. Fossil-bearing and carbonaceous shales, identified during the petrographic study of thin sections, were not analyzed

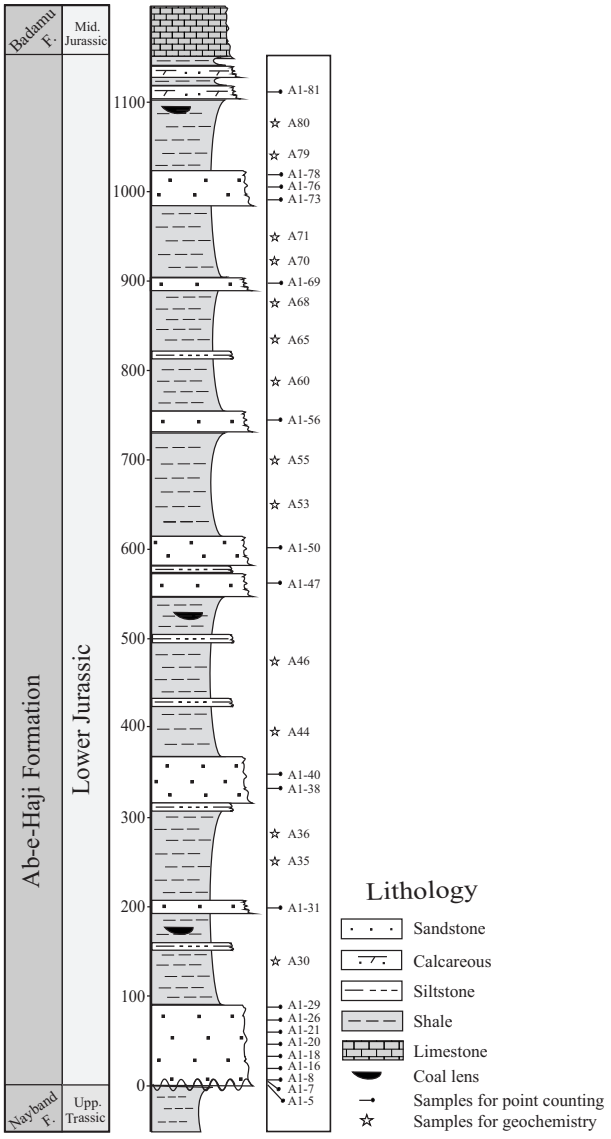

Figure 2. Lithostratigraphic section of the Ab-e-Haji Formation showing the location of samples.

in order to minimize the effect of carbonate on major elements concentrations (*e.g.*, Cullers, 2000) and of organic matter on mobilization of trace elements (*e.g.*, Lev *et al.*, 2008). Analyses were performed by inductively coupled plasma-mass spectrometry (ICP-MS) and inductively coupled plasma-atomic emission spectroscopy (ICP-AES) at the SGS Laboratory in Toronto, Canada.

The mineral and geochemical data were processed with the DODESSYS software (Verma and Díaz-González, 2012), which, for the identification and separation of discordant outliers, uses new precise and accurate critical values of Verma and Quiroz-Ruiz (2008, 2011) and Verma *et al.* (2008). The use of the mean and standard deviation as unbiased estimates of central tendency and dispersion parameters requires that the outlying observations be properly identified and separated (Verma, 2012), for which a suitable computer program DODESSYS has been recently available. The use of precise and accurate critical values renders the statistical inferences much more reliable than the older less precise values (see Verma, 2005, for a compilation of older values and the explanation of discordant outlier procedures). This software by Verma and Díaz-González (2012) provides a summary of all statistical information in an efficient way and has been especially recommended for use in geosciences. Only single-outlier type discordancy tests (Verma, 1997; Verma *et al.*, 2009) were applied at a strict confidence level of 99% to separate rarely one or two discordant outliers, and the final statistics (mean and standard deviation values) were computed from DODESSYS. For most parameters, no discordant outliers were actually detected by this software whereas for some elements, only one or at most two discordant observations were separated. This implies a good quality of the experimental data (both field sampling and laboratory analysis). The statistical information (mean and standard deviation) were reported as rounded values after Bevington and Robinson (2003) and Verma (2005).

RESULTS

Sandstone petrography

Ab-e-Haji sandstones are grain-supported, moderately sorted sandstones consisting mainly of sub-rounded to rounded grains. The main constituents are quartz grains (51.18%) and labile lithic fragments (48.15%), as well as feldspar (1.68%), which is a compositional characteristic of immature sandstones.

Monocrystalline quartz grains mainly show undulose extinction (Figure 3a), whereas polycrystalline quartz have extremely undulatory extinction and contain subcrystals with crenulated to suture boundaries (Figure 3b; probably derived from a metamorphic source rock; Krynine, 1940; Folk, 1980; Asiedu *et al.*, 2000). Also, quartz grains bearing individual domains with apparent bends (Figure 3c) were observed in sandstone samples as evidence of deformed parent rock for these sandstones (Passchier and Trouw, 2005).

Feldspars are present in low abundance and comprise rarely microcline (Figure 3d) and weathered orthoclase, which commonly have smaller size than quartz.

The Ab-e-Haji sandstones contain a considerable amount of rock fragments including metasedimentary and sedimentary types. The metamorphic rock fragments are metapelite grains, dominantly slate grains with slaty cleavage (Figure 3e) and phyllitic quartzite lithics containing re-crystallized micas in preferred planar orientation (Figure 3f) (Dorsey, 1988). Sedimentary lithics are mostly shale, chert and sandstone (Figure 3g). Moreover, fine to very fine zircon and tourmaline grains were observed in these deposits (Figure 3h).

Modal analysis

Table 1 lists modal compositional data (both actually measured grain counts and percentages) and their statistical synthesis for 20 samples of Ab-e-Haji sandstone. The recalculated modal data for the ternary diagrams (Figure 4) are also included in Table 1. On the basis of the Gazzi-Dickinson point-count method (Gazzi, 1966; Dickinson, 1970), and the sands classification of Dickinson (1985), Ab-e-Haji sandstones show quartzolithic nature (Qm_{38}-F_2-Lt_{60}, Qt_{58}-F_2-L_{40}; see statistical information in Table 1). Also, plotting of the modal analysis data of the sandstones in the basic ternary Qm-F-Lt and Qt-F-L diagram (Dickinson *et al.*, 1983) shows transitional recycled and recycled orogen tectonic provenance, respectively (Figures 4a, 4b). According to Dickinson (1985), sediments that originate from recycled orogens include various proportions of materials whose compositions reflect ultimate derivation from different sources. Variation in sedimentary rock fragments (shale, siltstone, sandstone and chert) as well as low grade metamorphic rock fragments (slate and phyllite) in the studied samples, point to derivation of clastic grains from fold-thrust belts (Dickinson and Suczek, 1979; Franzinelli and Potter, 1983; Dickinson, 1985).

Furthermore, diagrams based on the proportion of lithic fragments ($Lm_{86.97}$-Lv_0-$Ls_{13.03}$, $Qp_{33.58}$-Lvm_0-$Lsm_{72.09}$) (Ingersoll and Suczek, 1979; Dickinson and Suczek 1979) indicate the evolution of a suture tectonic zone and growth of fold-thrust belts in provenance terrain of Ab-e-Haji depositional basin (Figure 4c, 4d). Such a provenance tectonic setting can be consistent with the Eo-Cimmerian orogenic phase related to central Iran-Eurasia continental collision at the end of the Triassic. In addition, labile fragments derived from a fold-thrust belt could deposit in a nearby foreland basin as already mentioned by Aghanabati (2004) for the depositional basin of the Shemshak Group (comprising the Ab-e-Haji Formation).

However, the rare presence of potassium feldspars (orthoclase and microcline), especially at the upper parts of the section (van Hattum *et al.*, 2006) as well as the presence of zircon and tourmaline, may imply minimal inputs from a felsic plutonic source during the latest stages of Ab-e-Haji sandstone deposition.

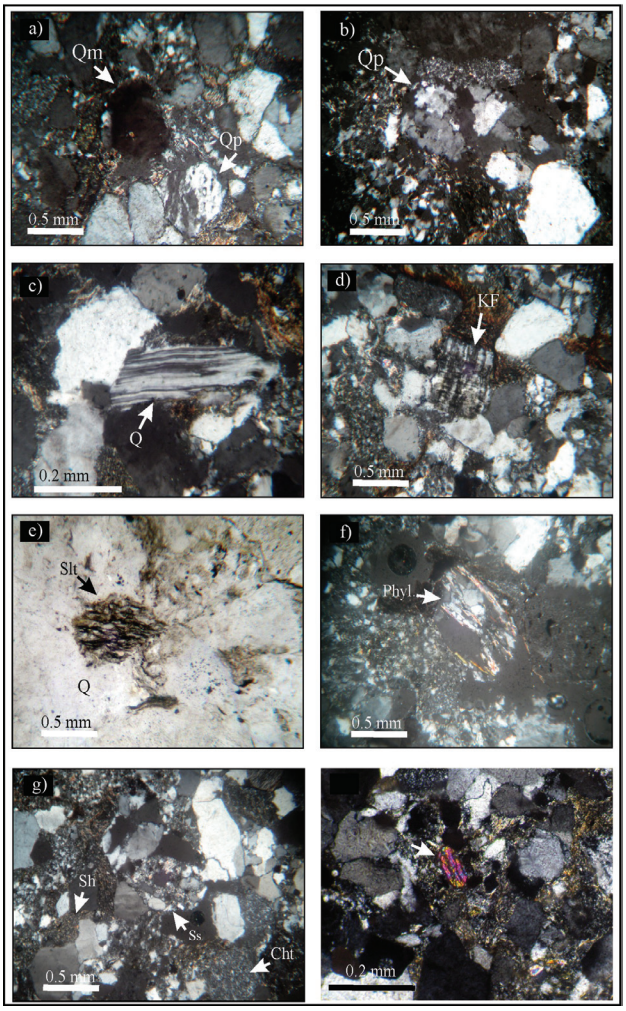

Figure 3. Photomicrographs of representative sandstones of Ab-e-Haji Formation (all with crossed-polarized light, except for e). a: Monocrystalline quartz with undulose extinction (sample A1.8). b: Polycrystalline quartz grains with crenulate to suture contact between subgrains (sample A1.21). c: Quartz grain bearing individual fibers with apparent bends (sample A1.47). d: Weathered potassium feldspar, microcline (sample A1.76). e: Lithic of slate with slaty cleavage (sample A1.56). f: Phyllitic quartzite lithics containing recrystallized micas (sample A1.40). g: Lithics of chert, sandstone and shale (sample A1.47). h: Fine-grained zircon in a sandstone sample. (Q): Quartz, (Qm): Monocrystalline quartz, (Qp): Polycrystalline quartz, (KF): potassium feldspar, (Slt): slate, (Phyl): Phyllit, (Cht): Chert, (Ss): sandtstone, (Sh): shale.

Elemental variation

The compositional data for major and trace elements including rare earth elements (REE) for fourteen shale samples from the study area are listed in Tables 2 and 3. Also included in these tables are the lower limits of detection (LOD) data for these elements. Many of the LOD values (Table 3) are consistent with the quality parameter of odd-even effect proposed by Verma *et al.* (2002) and Verma and Santoyo (2005). In fact, these LOD values should be estimated to at least two significant digits as suggested by these authors. Nevertheless, the LOD values give an indication of the quality of major and trace element data presented in this work.

According to SiO_2/Al_2O_3 vs. Fe_2O_3/K_2O ratios in Herron diagram (Herron, 1988) (Figure 5) most of the analyzed samples plot in the Fe-shale field, and few in the Fe-sand field. Shift of a few samples into the Fe-sand field probably results from variations in SiO_2 content from shale to silty-shale Fe-rich samples.

In comparison with Post-Archean Australian Shale (PAAS; representative continentally derived sediments) (Taylor and McLennan 1985), Ab-e-Haji shales show

Table 1. Modal analysis of sandstone samples from the Ab-e-Haji Formation, Iran.

Sample no.	Qm	Q>3	Q2-3	Cht	Ls	Lv	Lm	K	P	Acc	M	Sum	Qt	F	Lt	L	Qp
A1-5	90	38	10	19	15	0	94	4	0	1	36	307	157	4	176	109	67
A1-7	78	42	5	29	19	0	103	6	0	0	19	301	154	6	198	122	76
A1-8	103	28	1	25	17	0	110	6	0	1	17	308	157	6	181	127	54
A1-16	101	37	3	21	19	0	95	7	0	0	23	306	162	7	175	114	61
A1-18	97	21	1	20	5	0	104	7	0	1	45	301	139	7	151	109	42
A1-20	122	19	3	18	5	0	92	4	0	1	44	308	162	4	137	97	40
A1-21	104	35	4	16	12	0	91	5	0	1	32	300	159	5	158	103	55
A1-26	110	33	2	22	16	0	96	3	0	0	26	308	167	3	169	112	57
A1-29	99	30	1	17	11	0	103	5	0	0	38	304	147	5	162	114	48
A1-31	94	27	3	18	18	0	99	4	0	1	41	305	142	4	165	117	48
A1-38	108	34	4	21	13	0	88	2	0	2	29	301	167	2	160	101	59
A1-40	109	25	2	25	20	0	85	4	0	1	33	304	161	4	157	105	52
A1-47	117	36	5	19	14	0	91	1	0	0	23	306	177	1	165	105	60
A1-50	95	39	5	28	8	0	81	3	0	1	40	300	167	3	161	89	72
A1-56	103	25	2	22	15	0	93	4	0	0	44	308	152	4	157	108	49
A1-69	93	31	2	29	7	0	103	2	0	2	32	301	155	2	172	110	62
A1-73	96	29	1	15	11	0	107	8	0	0	37	304	141	8	163	118	45
A1-76	117	24	2	18	19	0	87	2	0	2	29	300	161	2	150	106	44
A1-78	101	30	4	24	16	0	88	5	0	1	38	307	159	5	162	104	58
A1-81	103	31	6	23	26	0	85	9	0	3	34	320	163	9	171	111	60

												Ternary Qm-F-Lt			Ternary Qt-F-L		
Sample no.	**Qm%**	**Q>3%**	**Q2-3%**	**Cht%**	**Ls%**	**Lv%**	**Lm%**	**K%**	**P%**	**Acc%**	**M%**	**Qm**	**F**	**Lt**	**Qt**	**F**	**L**
A1-5	29.3	12.4	3.3$^{\delta}$	6.2	4.9	0	30.6	1.3	0	0.3	11.7	33.3	1.5	65.2	58.1	1.5	40.4
A1-7	25.9	14.0	1.7	9.6	6.3	0	34.2	2.0	0	0	6.3	27.7	2.1	70.2	54.6	2.1	43.3
A1-8	33.5	9.1	0.3	8.1	5.5	0	35.7	2.0	0	0.3	5.5	35.5	2.1	62.4	54.1	2.1	43.8
A1-16	33.0	12.1	1.0	6.9	6.2	0	31.0	2.3	0	0	7.5	35.7	2.5	61.8	57.2	2.5	40.3
A1-18	32.2	7.0	0.3	6.6	1.7	0	34.6	2.3	0	0.3	15	38.0	2.7	59.2	54.5	2.7	42.7
A1-20	39.6	6.2	1.0	5.8	1.6	0	29.9	1.3	0	0.3	14.3	46.4	1.5	52.1	61.6	1.5	36.9
A1-21	34.7	11.7	1.3	5.3	4	0	30.3	1.7	0	0.3	10.7	39.0	1.9	59.2	59.6	1.9	38.6
A1-26	35.7	10.7	0.6	7.1	5.2	0	31.2	1.0	0	0	8.5	39.0	1.1	59.9	59.2	1.1	39.7
A1-29	32.6	9.9	0.3	5.6	3.6	0	33.9	1.6	0	0	12.5	37.2	1.9	60.9	55.3	1.9	42.9
A1-31	30.8	8.9	1.0	5.9	5.9	0	32.5	1.3	0	0.3	13.4	35.7	1.5	62.7	54.0	1.5	44.5
A1-38	35.9	11.3	1.3	7.0	4.3	0	29.2	0.7	0	0.7	9.6	40.0	0.7	59.3	61.9	0.7	37.4
A1-40	35.9	8.2	0.7	8.2	6.6	0	28.0	1.3	0	0.3	10.8	40.4	1.5	58.1	59.6	1.5	38.9
A1-47	38.2	11.8	1.6	6.2	4.6	0	29.8	0.3	0	0	7.5	41.3	0.4	58.3	62.5	0.4	37.1
A1-50	31.7	13.0	1.7	9.3	2.7	0	27.0	1.0	0	0.3	13.3	36.7	1.2	62.2	64.5	1.2	34.4
A1-56	33.4	8.1	0.7	7.1	4.9	0	30.2	1.3	0	0	14.3	39.0	1.5	59.5	57.6	1.5	40.9
A1-69	30.9	10.3	0.7	9.6	2.3	0	34.2	0.7	0	0.7	10.6	34.8	0.7	64.4	58.1	0.7	41.2
A1-73	31.6	9.5	0.3	5.0	3.6	0	35.2	2.6	0	0	12.2	36.0	3.0	61.0	52.8	3.0	44.2
A1-76	39.0	8.0	0.7	6.0	6.3	0	29.0	0.7	0	0.7	9.6	43.5	0.7	55.8	59.9	0.7	39.4
A1-78	32.9	9.8	1.3	7.8	5.2	0	28.7	1.6	0	0.3	12.4	37.7	1.9	60.4	59.3	1.9	38.8
A1-81	32.2	9.7	1.9	7.2	8.1	0	26.6	2.8	0	0.9	10.6	36.4	3.2	60.4	57.6	3.2	39.2
*n**	20	20	19	20	20	---	20	20	---	20	20	20	20	20	20	20	20
Mean*	33.45	10.08	0.97	7.02	4.68	---	31.09	1.49	---	0.285	10.82	37.66	1.68	60.66	58.10	1.68	40.22
Standard deviation*	3.31	2.05	0.52	1.38	1.73	---	2.76	0.68	---	0.278	2.73	3.88	0.77	3.66	3.18	0.77	2.74

* Statistical information (*n*=number of discordant outlier-free samples; Mean and Standard Deviation of discordant outlier-free data) was obtained from DODESSYS software (Verma and Díaz-González, 2012) after the application of single-outlier type discordancy tests (Verma 1997; Verma *et al*., 2009). Discordant outlier is indicated by the symbol $^{\delta}$. The statistical information is reported as rounded values (less strict method) after Bevington and Robinson (2003) and Verma (2005).

Qm: monocrystalline quartz, Q2-3 and Q>3: polycrystaline quartz, Cht: chert, Ls: sedimentary lithic grains, Lv: volcanic lithic grains, Lm: metamorphic lithic grains, K: potassium feldspar, P: plagioclase, Acc: accessory minerals, M: Matrix. Qt= Qm +Qp, F: K+P, Lt = Qp+L, Qp = Q2-3+Q>3+Cht, L = Lv+Ls+Lm.

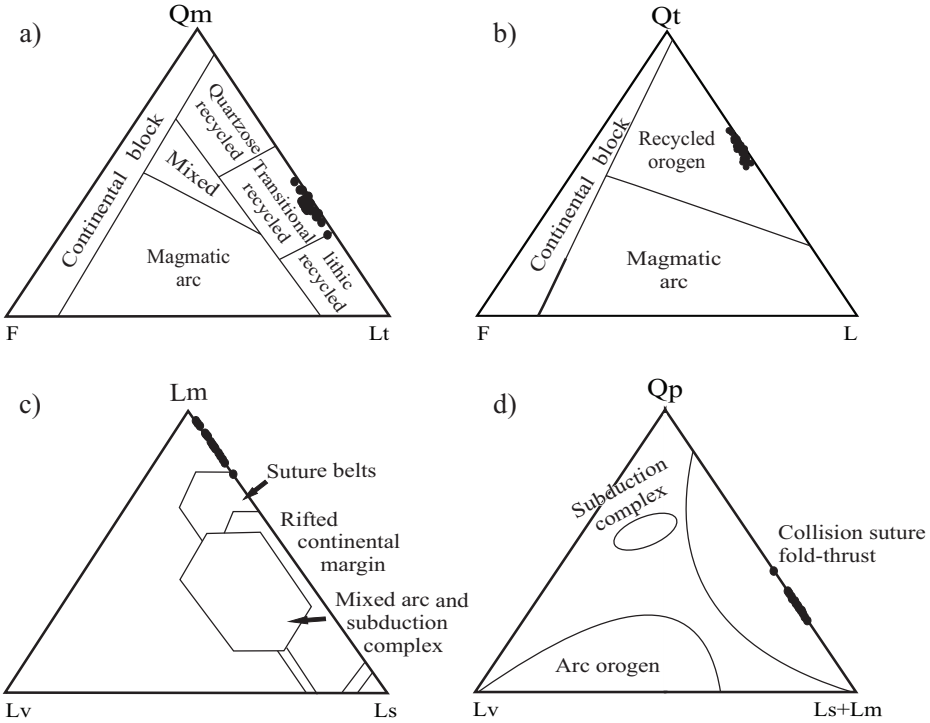

Figure 4. Modal composition of Ab-e-Haji sandstones in the ternary diagrams Qm-F-Lt (a) and Q_t-F-L (b) from Dickinson *et al*. (1983); Lm-Lv-Ls (c) from Ingersoll and Suczek (1979); and Qp-Lv-Ls+Lm (d) from (Dickinson and Suczek 1979). Abbreviations are defined in Table 1.

strongly depletion in constituents like Na_2O (0.3 times PAAS), CaO and MgO (0.5 times PAAS), and are moderately depleted in K_2O (0.7 times PAAS) and Al_2O_3 (0.8 times PAAS) (Figure 6).

On average, the samples show abundances of SiO_2 and TiO_2 similar to PAAS. The similarity of SiO_2 content in studied samples with PAAS implies that the observed depletion in CaO and Na_2O is not likely due to quartz dilution. However, because Ca and Na contents can be controlled by plagioclase, the depletion of these elements may reflect the lack of plagioclase in analyzed samples.

The K_2O content shows statistically significant correlation with Al_2O_3 ($r = 0.93$; $n = 14$), which indicates that K_2O abundance is controlled by clay minerals (Figure 7). Al_2O_3 content also shows a positive correlation with TiO_2 (0.80; Figure 7), which may suggest residual enrichment of these elements as a result of source area chemical weathering or alternatively, due to sorting (Lee, 2009).

In comparison to PAAS, variable degrees of depletion are clearly shown in large ion lithophile elements (Rb, Cs, Ba, Sr; 0.8, 0.4, 0.5, 0.5 times PAAS, respectively) and transition metal elements (Sc, V, Ni, Cr, Cu; 0.8, 0.8, 0.7, 0.6, 0.6 times PAAS, respectively), except for Co (1.1 times PAAS) (Table 3; Figure 8). The PAAS-normalized data show that shales are enriched in high field strength elements such as Hf and Zr (1.7 and 1.6 times PAAS, respectively), and have a similar content of Th relative to PAAS. In contrast Nb and U abundances are depleted to about 0.8 times PAAS.

Rb, Ba and Cs have a significant positive correlation coefficient with Al_2O_3 (0.95, 0.90 and 0.83, respectively; Figure 7), which may suggest that their distribution is significantly controlled by clays.

The variation in the abundance of transition metal elements in shales with the Al_2O_3 content is shown in Figure 7. The most significant correlations are those of Sc (0.92), V (0.90) and Ni (0.83), indicating that they are mainly concentrated in phyllosilicates.

The abundances and ratios of rare earth elements from the selected samples are shown in Tables 3 and 4. Studied samples are characterized by REE fractionation with an average $(La/Yb)_n$ ratio of 8.8. The light rare earth elements (LREE) are fractionated, $(La/Sm)_n$=3.8, and the heavy rare earth elements (HREE) patterns are almost flat, $(Gd/Yb_n$=1.5 (Figure 9). The ratio of LREE/HREE is (8.48) and the average of total rare earth element concentrations of Ab-e-Haji shales (202 ppm) is somewhat higher than that of PAAS (183 ppm). The europium anomaly is always negative, ranging from 0.60 to 0.69 (average 0.65). This characteristic is similar to that of PAAS (0.66).

DISCUSSION

Parent rocks

Major elements (Al_2O_3, TiO_2, Fe_2O_3, MgO, CaO, Na_2O, and K_2O) are used to discriminate four sedimentary provenances in the diagram of Roser and Korsch (1988):

Table 2. Major element concentrations in weight percent for shales of the Ab-e-Haji Formation.

Sample	SiO_2	TiO_2	Al_2O_3	$Fe_2O_3^t$	MnO	MgO	CaO	Na_2O	K_2O	P_2O_5	LOI	Sum
LOD	0.01	0.01	0.01	0.01	0.01	0.01	0.01	0.1	0.01	0.01	0.01	---
A30	64.0	1.16	18.5	4.63	0.04	1.49	0.34	0.2	3.36	0.08	6.28	100.08
A35	72.6	0.74	11.8	3.19	0.02	0.99	0.23	0.1	2.05	0.07	4.48	96.27
A36	71.4	0.89	13.5	3.42	0.02	0.98	0.24	0.2	2.55	0.07	4.73	98.00
A44	67.6	1.01	16.3	2.90	0.03	0.92	0.38	0.2	2.56	0.07	6.1	98.07
A46	64.0	0.94	15.3	5.42	0.03	0.85	0.36	0.2	2.37	0.07	6.41	95.95
A53	72.1	0.92	10.5	1.89	0.02	0.53	0.26	0.1	1.44	0.04	4.83	92.63
A55	62.7	1.09	19.8	3.10	0.02	1.15	0.36	0.3	3.22	0.08	7.44	99.26
A60	62.7	0.88	15.3	6.25	0.12	1.18	0.43	0.2	2.61	0.14	6.69	96.50
A65	69.9	0.95	14.8	3.43	0.07	0.93	0.35	0.2	2.42	0.07	5.48	98.60
A68	67.1	0.95	15.5	4.99	0.09	1.06	0.42	0.2	2.53	0.10	6.26	99.20
A70	70.4	0.95	14.1	3.28	0.04	0.89	0.29	0.2	2.25	0.06	5.26	97.72
A71	75.1	0.68	10.6	3.51	0.04	0.92	0.24	0.8	1.91	0.07	3.72	97.59
A79	58.2	0.87	16.5	5.11	0.04	1.57	3.22	0.6	3.04	0.17	8.09	97.41
A80	64.0	0.93	15.1	4.84	0.08	1.36	1.20	0.8	2.61	0.12	5.73	96.77
	$(SiO_2)_{adj}$	$(TiO_2)_{adj}$	$(Al_2O_3)_{adj}$	$(Fe_2O_3^t)_{adj}$	$(MnO)_{adj}$	$(MgO)_{adj}$	$(CaO)_{adj}$	$(Na_2O)_{adj}$	$(K_2O)_{adj}$	$(P_2O_5)_{adj}$		
A30	68.23	1.24	19.72	4.94	0.043	1.59	0.36	0.21	3.58	0.09		
A35	79.09	0.81	12.86	3.48	0.022	1.08	0.25	0.11	2.23	0.08		
A36	76.55	0.95	14.47	3.67	0.021	1.05	0.26	0.21	2.73	0.08		
A44	73.50	1.10	17.72	3.15	0.033	1.00	0.41	0.22	2.78	0.08		
A46	71.48	1.05	17.09	6.05	0.034	0.95	0.40	0.22	2.65	0.08		
A53	82.12	1.05	11.96	2.15	0.023	0.60	0.30	0.11	1.64	0.05		
A55	68.29	1.19	21.56	3.38	0.022	1.25	0.39	0.33	3.51	0.09		
A60	69.81	0.98	17.04	6.96	0.134	1.31	0.48	0.22	2.91	0.16		
A65	75.06	1.02	15.89	3.68	0.075	1.00	0.38	0.21	2.60	0.08		
A68	72.20	1.02	16.68	5.37	0.097	1.14	0.45	0.22	2.72	0.11		
A70	76.14	1.03	15.25	3.55	0.043	0.96	0.31	0.22	2.43	0.06		
A71	80.00	0.72	11.29	3.74	0.043	0.98	0.26	0.85	2.03	0.07		
A79	65.16	0.97	18.47	5.72	0.045	1.76	3.61^{δ}	0.67	3.40	0.19		
A80	70.30	1.02	16.59	5.32	0.088	1.49	1.32^{δ}	0.88	2.87	0.13		
*n**	14	14	14	14	14	14	12	14	14	14		
Mean*	73.4	1.011	16.19	4.37	0.051	1.155	0.354	0.335	2.72	0.095		
Standard deviation*	5.0	0.131	2.88	1.35	0.034	0.301	0.078	0.261	0.55	0.039		

The subscript $_{adj}$ refers to 100% adjusted data. For statistical information (*) and the symbol $^{\delta}$, see explanation in Table 1.

mafic igneous (P1); intermediate (P2); felsic (P3); and quartzose recycled (P4). In this diagram, the majority of the Ab-e-Haji samples plot in the P4 field, except for two samples (from the upper part of the section), which plotted in the P3 field (Figure 10). Also, plotting geochemical data in La–Th–Sc compositional space (Figure 11), strongly indicates that these sediments were derived from a mixed sedimentary or (meta)sedimentary source (Cullers, 1994a, 1994b). These results indicate a role of recycled sources in the deposition of Ab-e-Haji Formation, which at the upper part of the section were probably mixed with a minor felsic source.

Transition metal elements are compatible in magmatic processes and are more concentrated in mafic than silicic igneous rocks (Cullers, 1995). Depletion of transition metals (Cu, Sc, Ni, Cr, and V, except Co) with respect to PAAS can be explained as the result of sediment derivation from a more silicic and fractionation source than the PAAS (Joo *et al.*, 2005). Slight Co enrichment (1.1 times PAAS) in samples may suggest some input of mafic materials from the source area. Nevertheless, simultaneous depletion of all transition metals except Co shows that other factors, such as post-depositional alteration, might have controlled the Co concentration in the sediments (Osae *et al.*, 2006).

Chondrite-normalized REE abundances and patterns in Ab-e-Haji samples are generally similar to those of PAAS, which implies homogenization of these sediments (LREE enrichment, flat HREE and negative Eu). The europium anomaly 0.60 to 0.69 (average 0.65) indicate strong depletion of europium relative to neighboring rare earth elements, typical for PAAS as evidence for differentiated parent rocks (Taylor and McLennan, 1985). Furthermore,

Table 3. Trace and rare earth elements concentrations in ppm for shales of the Ab-e-Haji Formation.

	Sample																	
	LOD	**A30**	**A35**	**A36**	**A44**	**A46**	**A53**	**A55**	**A60**	**A65**	**A68**	**A70**	**A71**	**A79**	**A80**	***n****	**Mean***	**S.D.***
Ba	1	491	291	327	342	312	233	457	415	357	340	306	231	364	308	14	341	74
Cu	0.5	29.5	29.4	33.8	26.9	26	19.4	38.1	34.7	31.2	31.2	30.1	19.7	27.8	23	14	28.6	5.4
Li	1	65	41	35	54	43	39	66	55	45	49	44	28	83	49	14	49.7	14.2
Ni	0.5	48.8	35.3	39.2	35.3	28.4	25	59.5	39.2	37.8	42.7	40.9	27.8	45	35.2	14	38.6	9
Sr	0.5	89.7	53.2	57.9	120	113	87.1	147	106	95.1	111	92.5	66.9	171	109	14	101.4	32.2
Ti	0.01	0.57	0.35	0.45	0.46	0.43	0.48	0.61	0.5	0.47	0.49	0.48	0.35	0.49	0.5	14	0.474	0.07
V	2	141	87	101	107	107	81	151	127	103	121	105	78	154	117	14	112.9	24
Zn	1	95	98	66	90	101	62	101	103	90	94	95	97	122	85	14	92.8	14.9
Co	0.1	26.8	67.5$^{\delta}$	11.5	24.6	24.3	23.7	16.2	21.5	38.6	24	12.5	20.4	21.3	23.1	13	22.2	6.8
Ga	0.1	27.6	16.6	19.7	23	20.8	14.2	27.8	22.6	20.4	21.7	19.8	14.1	24.5	21.1	14	20.99	4.17
Hf	1	11	9	10	8	7	11	6	8	9	8	10	9	6	8	14	8.57	1.6
In	0.02	0.06	0.05	0.04	0.07	0.06	0.05	0.09	0.07	0.06	0.06	0.06	0.04	0.07	0.06	14	0.06	0.013
U	0.05	2.75	1.98	2.23	2.39	2.56	2.51	3.05	2.59	2.22	2.37	2.2	1.71	2.2	2.01	14	2.341	0.342
Cs	0.1	6.7	4.6	3.5	7.1	6.3	3.8	8.1	5.9	5.2	6.2	5.7	5.1	7.9	6	14	5.864	1.364
Mo	0.05	0.59	0.75	1.93$^{\delta}$	0.28	0.31	0.46	0.54	0.5	0.47	0.55	0.44	0.31	0.31	0.24	13	0.442	0.148
Nb	0.1	18.4	4	17.8	11	10	10.5	27.8	18.2	13.5	17	17.8	8.3	20	19.4	14	15.3	6.1
Pb	0.5	6.6	17	5.1	18.2	20.2	14.8	20.3	20.4	18.7	19.9	17.1	21	17.3	16.8	14	16.7	4.9
Rb	0.02	171	110	125	146	133	78.6	175	143	123	135	121	93.3	174	138	14	133.3	28.5
Sb	0.05	0.29	0.15	0.17	0.16	0.12	0.43	0.4	0.37	0.34	0.38	0.31	0.36	0.44	0.44	14	0.311	0.115
Sc	0.1	13.7	9.5	10.7	12.6	12.2	9	16.2	14.5	11	12.9	11	8.6	14.8	12.4	14	12.08	2.26
Sn	0.3	3.6	2.2	2.8	3	2.7	2.2	3.9	3	2.7	2.8	2.6	1.8	3	2.6	14	2.78	0.54
Ta	0.05	1.5	0.38	0.9	0.21	0.24	0.62	1.84	1.1	0.91	1.09	0.63	0.37	1.13	1.2	14	0.866	0.49
Tb	0.05	0.73	0.57	0.59	0.62	0.66	0.56	0.8	0.69	0.58	0.66	0.61	0.46	0.77	0.65	14	0.639	0.09
Zr	0.5	431	354	392	282	285	411	208	294	348	305	380	366	219	303	14	327	68
Th	0.2	17.5	11.2	13.1	14.2	12.7	11.9	16.4	13.5	12.7	13.3	13.2	8	13	12.5	14	13.09	2.21
Tl	0.02	0.77	0.47	0.57	0.58	0.51	0.34	0.73	0.6	0.48	0.53	0.48	0.36	0.59	0.49	14	0.536	0.119
W	0.1	130	403$^{\delta}$	4.7	19.5	38.8	88.5	46	86.7	240	118	2.7	88.3	52.4	89.3	13	77	64
Y	0.1	16.4	12.6	13.4	15.3	17.1	13.7	18.8	16.1	13.8	16.2	14.3	11.6	18.6	15.8	14	15.26	2.14

S.D. Standard deviation. For statistical information (*) and the symbol $^{\delta}$, see explanation in Table 1.

the high LREE/HREE ratio (8.48) of Ab-e-Haji shales is characteristic of felsic source rocks (Taylor and McLennan, 1985; Wronkiewicz and Condie, 1989, Cullers, 1994b).

Higher mean contents of the REE in studied samples (202 ppm) relative to PAAS (183 ppm) could be the result of a higher degree of weathering and sedimentary recycling, or even probably due to the relatively higher abundances of REE-bearing heavy minerals. However, caution is required in comparing mean values without reference to a dispersion parameter such as the standard deviation; in fact, significance tests should be applied in future to ascertain these interpretations (Verma, 2009). Unfortunately, estimates of the dispersion parameter are lacking for the average upper continental crust (Taylor and McLennan, 1985).

Moderate to low correlation coefficient between ΣREE, LREE and HREE and Al_2O_3 (0.78, 0.78, 0.66, respectively) suggests that other phases, in addition to clay minerals, might control the REE concentration.

Statistically insignificant negative correlation between Zr and (Gd/Yb)n probably indicates that the HREE fractionation is not controlled by zircon, which is also in agreement with the low correlation of Zr with HREE. The statistically significant correlation of ΣREE, LREE and HREE with TiO_2 (0.92, 0.88, 0.90, respectively) implies the occurrence of some Ti-bearing oxides, which may probably host REE (González-López *et al.*, 2005).

Generally, the LREE enrichment, negative Eu anomaly and almost flat HREE pattern may indicate a cratonic source rock with the presence of felsic and (meta)sedimentary components (Gu *et al.*, 2002; Das *et al.*, 2006).

This is consistent with the ratios of trace elements that have not been seriously affected by secondary processes like diagenesis and metamorphism, and provide significant information about the provenance of sedimentary rocks (Taylor and McLennan, 1985; Condie and Wronkiewiez, 1990, Armstrong-Altrin *et al.*, 2004). La/Sc, Th/Cr and Th/Sc ratios of Ab-e-Haji sediments are within the range of fine-grained sediments derived from silicic sources (Cullers, 2000) (Table 4). In comparison, La/Sc (1.5×PAAS), La/Ni (1.6×PAAS), La/Th (1.2×PAAS), Th/Cr (1.7×PAAS), Th/Sc (1.2×PAAS) ratios are greater than those from PAAS (Table 4), suggesting that Ab-e-Haji samples were derived from falsic rocks and/or recycled sediments.

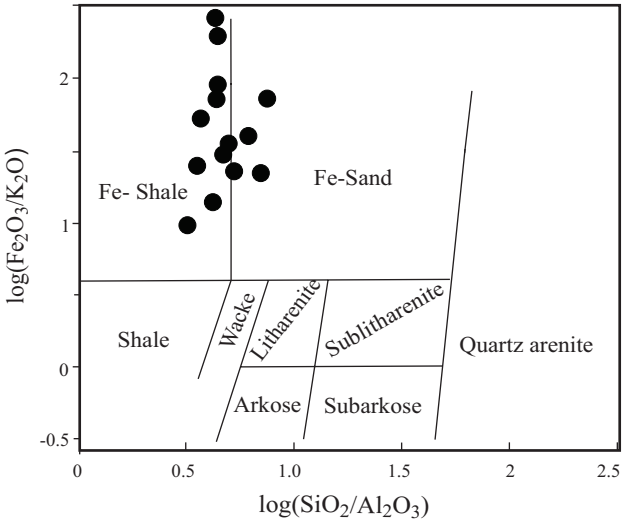

Figure 5. Classification of the Ab-e-Haji shales according to Herron (1988) diagram.

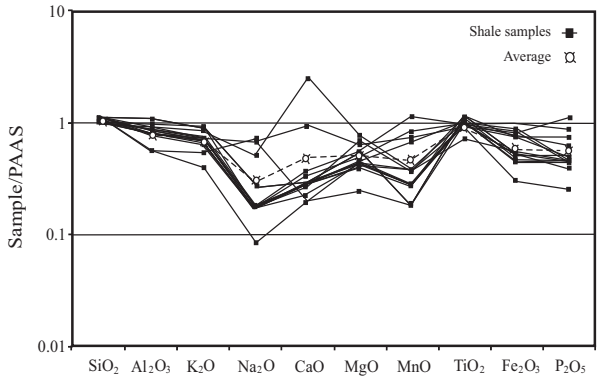

Figure 6. Post-Archean Australian Shale (PAAS)-normalized average major element composition for Ab-e-Haji shales. PAAS data from Taylor and McLennan (1985).

Paleoweathering and paleoclimate

Weathering effects are evaluated in terms of the molar percentage of the oxide components using the formula of the Chemical Index of Alteration (CIA= Al_2O_3 / (Al_2O_3 + CaO* + Na_2O + K_2O); Nesbitt and Young, 1982) where CaO* represents Ca in siliciclastic-bearing minerals only.

The CIA value of the Ab-e-Haji samples range from 71 to 83 (average 80), reflecting intermediate to extreme chemical weathering (Nesbitt and Young, 1982). This implies more intense weathering than average PAAS shale (69) or, alternatively, the presence of compositionally mature alumina-rich minerals produced by sedimentary recycling processes.

The weathering trend can also be illustrated on an Al_2O_3–CaO+Na_2O–K_2O (A–CN–K) triangular plot, which is useful for evaluating and correcting the effects of K-metasomatism and for giving some information of the composition of the fresh source rock (Nesbitt and Young, 1984; Fedo *et al.*, 1995). Plots of Ab-e-Haji samples on these diagrams show two different trends (Figure 12). The first one (samples with CIA values of 80 to 83) follows a trend towards the A-apex (near the illite composition), which indicates a high degree of alteration (Cingolani *et al.*, 2003).

The second one (samples with CIA values of 71 and 74) shows an almost parallel trend to the A–CN joint nearby the PAAS value. The solid line joining these data can be extended back to the plagioclase–alkali feldspar join. The intersection suggests a high plagioclase to alkali feldspar ratio in the source such as that found in tonalite. In this case, deviation of samples (dashed line) from the inferred weathering line of tonalite (solid line with arrow) can be due to K-metasomatism of weathered rocks (Fedo *et al.*, 1995).

Eventually, the high values of CIA (80-83) for most samples and their position in A–CN–K diagram could have been inherited from recycled sediments. Further, variation of individual CIA (71 to 83) and two different weathering trends in A–CN–K diagram may indicate the mixing of fine-grained sediments from two different source rocks (Condie *et al.*, 2001; Lee, 2002).

Also, large ion lithophile elements behave similar to related major elements during weathering processes. In stud-

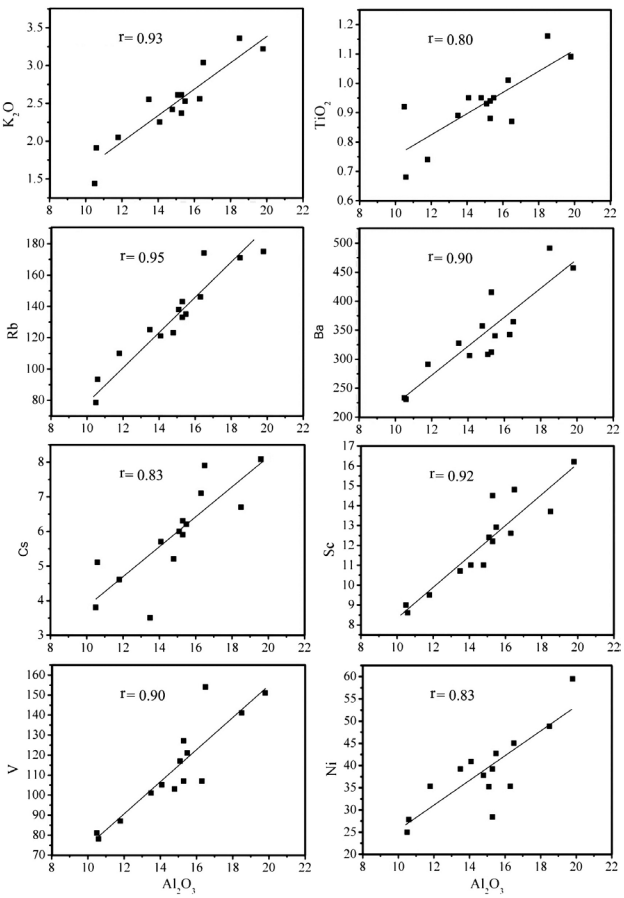

Figure 7. Selected major and trace elements versus Al_2O_3 graph showing the distribution of shale samples from the Ab-e-Haji Formation. Major element contents in wt. %; trace element contents in ppm).

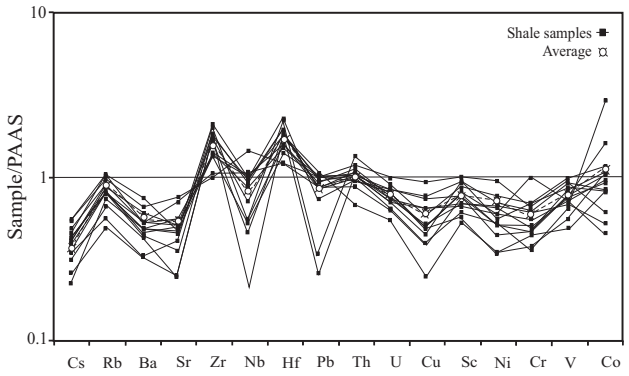

Figure 8. Post-Archean Australian Shale (PAAS)-normalized trace element composition of the Ab-e-Haji shales. PAAS data from Taylor and McLennan (1985).

ied samples, all large ion elements show depletion. Among alkali elements, Rb content is closer to PAAS (Figure 8), probably due to its less mobility (Das *et al.*, 2006). Ba, Rb, Cs and Sr are constituent elements of feldspars (Ohta, 2004) and thus, depletion of these elements in studied samples indicates low abundance of feldspar. Nevertheless, intense weathering and recycling is more probable, and is supported by depletion of K, Ca, Na, Mg, and Mn and high values of CIA in most samples from Ab-e- Haji shales.

In addition, the positive correlation of Rb with Ba (r=0.87) indicates their similar geochemical behavior. Rb and Ba also show positive correlation with K_2O (r=0.97 and 0.90, respectively) and Al_2O_3 (r=0.95 and 0.90, respectively; Figure 7). These relationships also imply that their distribution may be linked to illitic phases (Bauluz *et al.*, 2000; González-López *et al.*, 2005). The fine siliciclastics derived from intense chemical weathering, concomitant with recycling of older sediments, generally contain a high proportion of illite (Potter *et al.*, 1980; Lee, 2002).

The characteristics of clastic grains (Kutterolf *et al.*, 2008), such as major components ratios, and the climatic-discrimination diagram (Suttner and Dutta 1986) suggest a dominance of semi-humid climatic conditions for the source area of the Ab-e-Haji sandstones (Figure 13). This is in agreement with moderate to high values of weathering indexes, calculated from geochemical analysis. Moreover, the semi-humid climate, inferred from the composition of Ab-e-Haji sandstones, is supported by the presence of scattered coal seams in the studied section and from the paleogeographic location of central Iran, including the Tabas block, nearly above N30° during Jurassic times (Golonka and Ford, 2000).

However, the high abundance of labile rock fragments (metamorphic and sedimentary) in the Ab-e-Haji sandstones is in conflict with a semi-humid climate. In fact, under normal weathering conditions, lithic fragments are very susceptible to chemical weathering and can be easily destroyed during transport (Cameron and Blatt, 1971; Suttner *et al.*, 1981; Mehring and McBride, 2007). Thus, the abundance of labile lithic fragments in the studied sandstones probably indicates short sediment transport (Folk, 1980; Suttner *et al.*, 1981; Pettijohn *et al.*, 1987; Bauluz *et al.*, 2000).

Compositional maturity

The Index of Compositional Variability, ICV= $(Fe_2O_3+K_2O+Na_2O+CaO+MgO+TiO_2)/Al_2O_3$) and the K_2O/Al_2O_3 ratio (Cox *et al.*, 1995) of fine siliciclastic rocks can be used to quantify the compositional maturity. In general, the ICV value lower than one for the Ab-e-Haji samples (average=0.63) indicates a tectonically quiescent environment, where recycling and weathering are active (Weaver, 1989; Joo *et al.*, 2005).

Furthermore, ancient fine-grained sediments with K_2O/Al_2O_3 ratios less than 0.4 point to minimal alkali feldspar abundance relative to other minerals in the original siliciclastics (Cox *et al.*, 1995). However, the analyzed

Table 4. Elemental ratios of Ab-e-Haji shales, fine-fractions derived from silicic and basic sources, upper continental crust and PAAS,

Elemental ratios	Average of Ab-e-Haji shales	Range of fine fractions from silicic sources[1]	Range of fine fractions from basic sources[1]	Upper continental crust[2]	PAAS[3]
La/Ni	1.1				0.69
La/Th	3.19				2.6
La/Sc	3.49	0.7 – 27.7	0.40 – 1.1	2.21	2.38
Th/Sc	1.09	0.64 – 18.1	0.05 – 0.4	0.79	0.91
Th/Cr	0.22	0.067 – 4.0	0.002 – 0.045	0.13	0.13
Th/Ni	0.35				0.27
Eu/Eu*	0.65	0.32 – 0.83	0.70 – 1.02		0.66
(La/Yb)n	8.8				9.2
(La/Sm)n	3.8				4.3
(Gd/Yb)n	1.5				1.4
∑REE	202.1				183

1: From Cullers (2000). 2: From Cullers *et al*. (1988). 3: Post-Archean Australian Shale from Taylor and McLennan (1985).

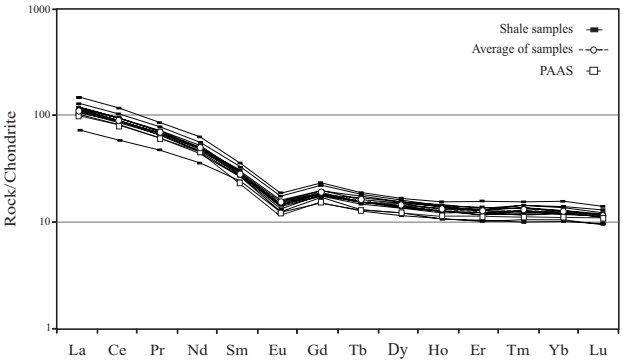

Figure 9. Chondrite-normalized REE patterns of Ab-e-Haji shales. Chondrite data from Taylor and McLennan (1985).

samples have an average ratio of K_2O/Al_2O_3 = 0.16, suggesting a low feldspar content. The dominance of low-grade metamorphic and sedimentary rocks in the source area, which have commonly low abundance of feldspar (Pettijohn *et al.*, 1987), may result in low values of K_2O/Al_2O_3 ratio in the studied shale samples.

Hydraulic sorting

Chemical composition of sedimentary rocks can be influenced by hydraulic sorting (Armstrong-Altrin, 2009). This process may control the distribution of some trace elements. In the studied shales, high values of linear correlation coefficient between Nb and Ta with Ti (0.87 and 0.84, respectively) suggest that these elements are hosted by accessory Ti-oxide phases (Taylor and McLennan, 1985). Also, they have higher Zr and Hf contents than the PAAS, and Zr has a strong correlation with Hf (r=0.98). Zr/Hf values range from 35 to 41, which are similar to the values reported for zircon crystals (Murali *et al.*, 1983). In the Th/Sc vs. Zr/Sc diagram of McLennan *et al.* (1993), the enrichment of Zr in the shales can be interpreted as the result of recycling processes (Figure 14), although depletion of Sc cannot be ruled out.

Regional constrains on tectonic provenance

During the Middle-Late Permian, Iran microplates, including the Tabas block, separated from the northern part of Gondwana and were attached to the southern margin of Laurasia in the Late Triassic. In the Iranian plate, this continent-continent collision resulted in a variety of phenomena such as deformation, metamorphism, regional unconformities and building up of the Cimmerian orogenic chain, with development of foreland basins (e.g, Zanchi *et al.*, 2009; Fursich *et al.*, 2009a, 2009b).

Moreover, a drastic shift in lithological facies from carbonate to thick clastic successions is another characteristic effect of this collision (Eo-Cimmerian orogeny; Seyed-Emami, 2003). In the Tabas block, this facies change can be detected by unconformable deposition of thick siliciclastic successions of the Shemshak Group, including the Nayband (Late Triassic) and Ab-e-Haji (Lower Jurassic) formations, over carbonate deposits of the Shotori Formation (Middle Triassic). Such a lithological change mostly points to a remarkable increase in availability of clastic sediments in the source area.

In this regard, the main uplift phase of the Eo-Cimmenrian orogeny at the Triassic-Jurassic boundary (Fursich *et al.* 2009a) provieded rejuvenation in the source area and therefore, the vast silicicalstics sources for Ab-e-Haji deposition. The fingerprints of these movements are recorded as Mississippi Valley Type (MVT) deposits in pre-Jurassic sediments (*e.g.,* Javanshir *et al.*, 2009). Noteworthy, the Ab-e-Haji sandstones contain labile rock fragments, produced by the exposure of low-grade metamorphic and

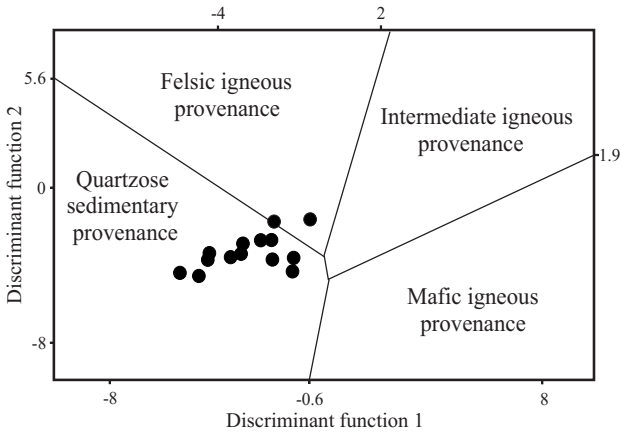

Figure 10. Discriminant function diagram for the provenance signatures of the Ab-e-Haji shales using major elements (Roser and Korsch 1988).

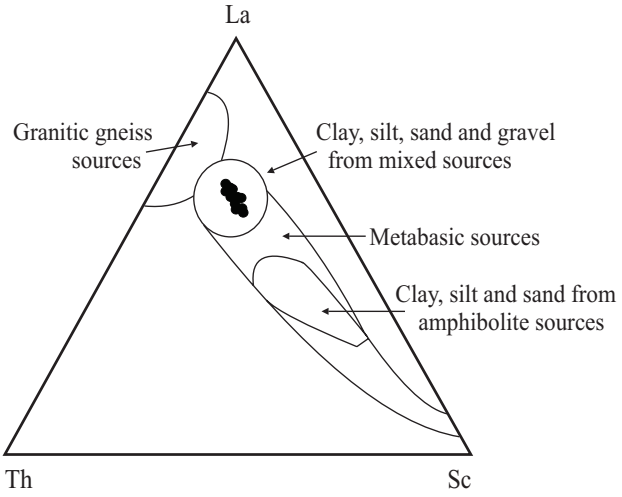

Figure 11. Plot of trace elements from Ab-e-Haji shales in La–Th–Sc compositional space (after Cullers 1994a).

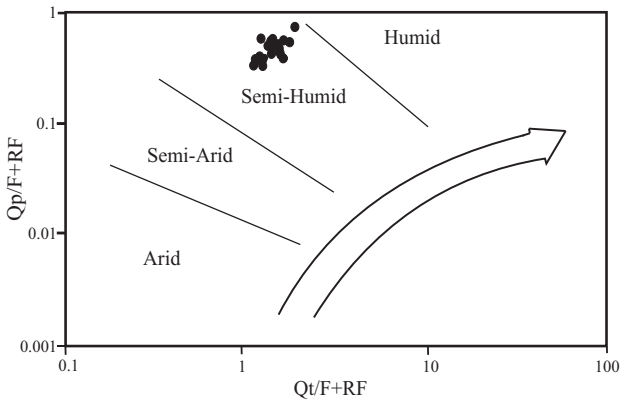

Figure 13. Ratios of major components of Ab-e-Haji sandstones in the climatic-discrimination diagram of Suttner and Dutta (1986). RF=Lv+Ls+Lm+Ch; Qp = Q2-3+Q>3+Cht; F= K+P; Qt=Qm +Qp.

sedimentary rocks, and indicative of a short transport path. Therefore, it is most probable that the displacement of intrabasinal faults such as the active Kuh-Banan basement fault, and exposure of supracrustal successions provided a mixed source rock area for the nearby Ab-e-Haji foreland basin.

CONCLUSIONS

Petrogarphic evidence such as the variation in sedimentary and low grade metamorphic rock fragments in the Ab-e-Haji sandstones, as well as provenance discrimination diagrams point to a derivation of these clastic grains from a recycled orogen related to a fold-thrust belt tectonic setting and to their deposition in a nearby foreland basin after short transport under semi-humid climatic conditions. Moreover, Ab-e-Haji shales are depleted in major and large ion lithophile elements in comparison to PAAS, which according to CIA values can be related to moderate to high weathering impact in the source area.

Major and trace element contents of shales in discriminating diagrams imply to role of recycled sources for the deposition of Ab-e-Haji Formation, which at the upper part of the section were probably mixed with a minor felsic source. In these samples transitional metal elements, such as Sc, V, and Ni are preferentially concentrated in clay minerals probably by surficial sorption. In addition, low content of these elements as well as element ratios such as La/Sc and Th/Sc, indicate the presence of fractionated source rocks with lower compatible element contents and recycled sediments in the source area. This result is consistent with the LREE enrichment, negative Eu anomaly and flat HREE pattern of these sediments that indicate a felsic and cratonic source with dominance of (meta)sedimentary rocks.

The Tabas block was influenced by the Eo-Cimmerain orgeny and consequently by local tectonic activity along the basement Kuh-Banan fault during late Triassic-lower Jurassic. Such a tectonic activity most probably controlled the lithological composition of outcrops in the source area of Ab-e-Haji foreland basin and the accessibility of huge source of silisiclastic sediments.

ACKNOWLEDGEMENTS

The manuscript was significantly improved from constructive comments and corrections by Prof. S.P. Verma. Also, we thank A. Abdi and H. Hooshmand Kouchi for their help during field work. We would like to thank Prof. E. Santoyo, associated editor of the RMCG and Prof. E. González Partida and anonymous reviewers for their helpful and constructive reviews.

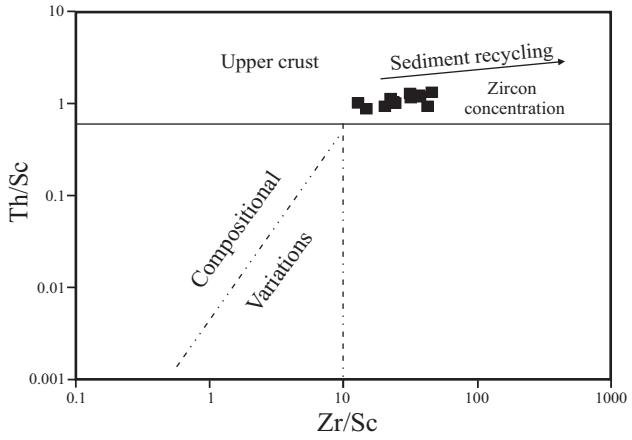

Figure 14. Th/Sc versus Zr/Sc diagram reflecting reworking and upper crust input (after McLennan *et al.*, 1993).

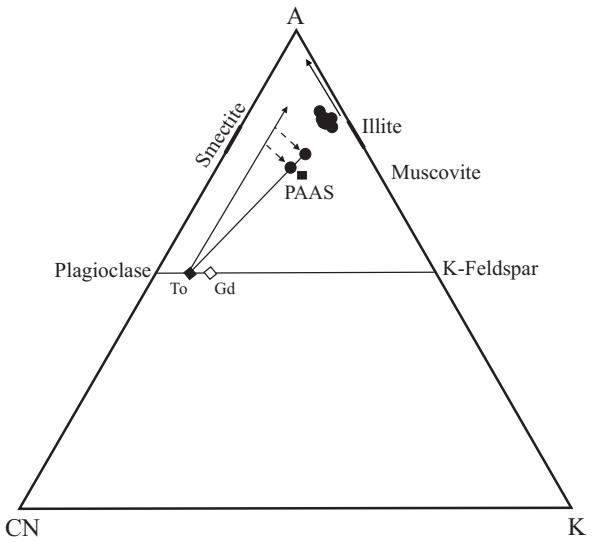

Figure 12. Al_2O_3–$CaO+Na_2O$–K_2O (A–CN–K) plot for the Ab-e-Haji shales (diagram after Nesbitt and Young, 1984). The proposed tonalite source is inferred from drawing a line through the two least altered samples. PAAS: Post-Archean Australian Shale; To: tonalite, Gd: granodiorite.

REFRENCES

Aghanabati, S. A., 2004, Geology of Iran (in Farsi): Tehran, Geological Survey of Iran Publication, 586 pp.

Alavi, M., Vaziri, H., Seyed-Emami, K., Lasemi, Y., 1997, The Triassic and associated rocks of the Nakhlak and Aghdarband areas in central and northeastern Iran as remnants of the southern Turan active continental margin: Geological Society of America Bulletin, 109, 1563-1575.

Armstrong-Altrin, J.S., 2009, Provenance of sands from Cazones, Acapulco, and Bahía Kino beaches, Mexico: Revista Mexicana de Ciencias Geológicas, 26(3), 764-782.

Armstrong-Altrin, J.S., Verma, S.P., 2005, Critical evaluation of six tectonic setting discrimination diagrams using geochemical data of Neogene sediments from known tectonic settings: Sedimentary Geology, 177, 115-129.

Armstrong-Altrin, J.S., Lee, Y.I., Verma, S.P., Ramasamy, S., 2004, Geochemistry of sandstones from the Upper Miocene Kudankulam Formation, southern India: implication for provenance, weathering and tectonic setting: Journal of Sedimentary Research, 74, 285-297.

Asiedu, D.K., Suzuki, S., Shibata, T., 2000, Provenance of sandstones from the Wakino Subgroup of the Lower Cretaceous Kanmon Group, northern Kyushu, Japan: The Island Arc, 9, 128-144.

Balini, M., Nicora, A., Berra, F., Garzanti, E., Levera, M., Mattei, M., Muttoni, G., Zanchi, A., Bollati, I., Larghi, C., Zanchetta, S., Salamati, R., Mossavvari, F., 2009, The Triassic stratigraphic succession of Nakhlak (Central Iran), a record from an active margin, *in* Brunet, M F., Wilmsen, M., Granath, J.W., (eds.), South Caspian to Central Iran Basins: London, The Geological Society, Special Publication 312, 287-321.

Bauluz, B., Mayayo, M.J., Fernández-Nieto, C., González-López J.M., 2000, Geochemistry of Precambrian and Paleozoic siliciclastic rocks from the Iberian Range, NE Spain: implications for source-area weathering, sorting, provenance, and tectonic setting: Chemical Geology, 168, 135-150.

Berberian, M., King, G.C.P., 1981, Towards a palaeogeography and tectonic evolution of Iran: Canadian Journal of Earth Sciences, 18, 210-265.

Bevington, P.R., Robinson, D.K., 2003, Data reduction and error analysis for the physical sciences: NewYork, Mc Graw Hill, 320 pp.

Bracciali, L., Marroni, M., Pandolfi, L., Rocchi, S., 2007, Geochemistry and petrography of Western Tethys Cretaceous sedimentary covers (Corsica and Northern Apennines): From source area to configuration of margins, *in* Arribas, J., Critlli, S., Johanson, M.J., (eds.), Sedimentary Provenance and Petrogenesis: Perspectives from Petrography and Geochemistry: Geological Society of America, Special Paper 420, 73-93.

Cameron, K.L., Blatt, H., 1971, Durabilities of sand-size schist and volcanic rock fragments during fluvial transport, Elk Creek, Black Hills, South Dakota: Journal of Sedmentary Petrology, 41, 565-576.

Cingolani, C.A., Manassero, M., Abre, P., 2003, Composition, provenance and tectonic setting of Ordovician siliciclastic rocks in the San Rafael block: Southern extension of the Precordillera crustal fragment, Argentina: Journal of South American Earth Sciences, 16, 91-106.

Condie, K.C., 1991, Another look at rare earth elements in shales: Geochimica et Cosmochimica Acta, 55, 2527-2531.

Condie, K.C., 1993, Chemical composition and evolution of the upper continental crust: contrasting results from surface samples and shales: Chemical Geology, 104, 1-37.

Condie, K.C., Wronkiewicz, D.J., 1990, A new look at the Archean-Proterozoic boundary: Sediments and the tectonic setting constraint, *in* Naqvi, S.M. (ed.), Precambrian Continental Crust and its Economic Resources: Amsterdam, Elsevier, 61-84.

Condie, K.C., Lee, D., Farmer, G.L., 2001, Tectonic setting and provenance of the Neoproterozoic Uinta Mountain and Big Cottonwood groups, northern Utah: constraints from geochemistry, Nd isotopes and detrital modes: Sedimentary Geology, 141-142, 443-464.

Cox, R., Low, D.R., Cullers, R.L., 1995, The influence of sediment recycling and basement composition on evolution of mudrock chemistry in the southwestern United States: Geochimica et Cosmochimica Acta, 59, 2919-2940.

Cullers, R.L., 1988, Mineralogical changes of soil and stream sediment formed by intense weathering of the Danburg granite, Georgia, U.S.A: Lithos, 21, 301-314.

Cullers, R.L., 1994a, The chemical signature of source rocks in size fractions of Holocene stream sediment derived from metamorphic rocks in the wet mountains region, Colorado, USA: Chemical Geology, 113, 327-343.

Cullers, R.L., 1994b, The controls on the major and trace element variation of shales, siltstones and sandstones of Pennsylvanian-Permian age from uplifted continental blocks in Colorado to platform sediment in Kansas, USA: Geochimica et Cosmochimica Acta, 58, 4955-4972.

Cullers, R.L., 1995, The controls on the major-and trace-element evolution of shales, siltstones and sandstones of Ordovician to Tertiary age in the Wet Mountains region, Colorado, USA: Chemical Geology, 123, 107-131.

Cullers, R.L., 2000, The geochemistry of shales, siltstones and sandstones of Pennsylvanian-Permian age, Colorado, USA: Implication for provenance and metamorphic studies: Lithos, 51, 181-203.

Cullers, R.L., Basu, A., Suttner, L., 1988, Geochemical signature of provenance in sand-size material in soils and stream sediments near the Tobacco Root batholith, Montana, USA: Chemical Geology, 70(4), 335-348.

Das, B.K., AL-Mikhlafi, A.S., Kaur, P., 2006, Geochemistry of Mansar Lake sediments, Jammu, India: Implication for source-area weathering, provenance, and tectonic setting: Journal of Asian Earth Sciences, 26, 649-668.

Davoudzadeh, M., Soffel, H., Schmidt, K., 1981, On the rotation of the Central-East Iran microplate: Neues Jahrbuch fur Geologie und Palaontologie, Monatshefte, 3, 180-192.

Dickinson, W.R. 1970, Interpreting detrital modes of greywacke and arkose: Journal of Sedimentary Petrology, 40, 695-707.

Dickinson, W.R., Suczek, C., 1979, Plate tectonics and sandstone composition: American Association of Petroleum Geologists Bulletin, 63, 2164-2182.

Dickinson, W.R., 1985, Interpreting provenance relation from detrital modes of sandstones, *in* Zuffa, G.G. (ed.), Provenance of Arenites: Dorderch, Holand, Reidel Publishing Company, 333-363.

Dickinson W.R., Beard L.S., Brakenridge G.R., Erjavec J.L., Ferguson R.C., Inman K.P., 1983, Provenance of North American Phanerozoic sandstones in relation to tectonic setting: Geological Society of American Bulletin, 94, 222-235.

Dorsey, R.J., 1988, Provenance evolution and unroofing history of a modern arc-continent collision: evidence from petrography of Plio-Pleistocene sandstones, eastern Taiwan: Journal of Sedimentary Petrology, 58, 208-218.

Etemad-Saeed, N., Hosseini-Barzi, M., Armstrong-Altrin, J.S., 2011, Petrography and geochemistry of clastic sedimentary rocks as evidences for provenance of the Lower Cambrian Lalun Formation, Posht-e-badam block, Central Iran: Journal of African Earth Sciences, 61, 142-159.

Fedo, C.M., Nesbitt, H.W., Young, G.M., 1995, Unraveling the effects of potassium metasomatism in sedimentary rocks and paleosols, with implications for paleoweathering conditions and provenance: Geology, 23, 921-924.

Folk, E., 1980, Petrography of sedimentary rocks: Hemphill Publishing Company, 182 pp.

Franzinelli, E., Potter, P.E., 1983, Petrology, chemistry and texture of modern river sands, Amazon River system: Journal of Geology, 91, 23-39.

Fursich, F.T., Hautmann, M., Senowbaridaryan, B., Seyed-Emami, K., 2005, The Upper Triassic Nayband and Darkuh formations of east-central Iran: Stratigraphy, facies patterns and biota of extensional basins on an accreted terrane: Beringeria, 35, 53-133.

Fursich, F.T., Wilmsen, M., Seyed-Emami, K., Majidifard, M.R., 2009a, Lithostratigraphy of the Upper Triassic-Middle Jurassic Shemshak

Group of Northern Iran, *in* Brunet, M.F., Wilmsen, M., Granath, J.W. (eds.), South Caspian to Central Iran Basins: London, The Geological Society, Special Publication, 312, 129-160.

Fursich, F.T., Wilmsen, M., Seyed-Emami, K., Majidifard, M.R., 2009b, The Mid-Cimmerian tectonic event (Bajocian) in the Alborz Mountains, Northern Iran: evidence of the break-up unconformity of the South Caspian Basin, *in* Brunet, M.F., Wilmsen, M., Granath, J.W. (eds.), South Caspian to Central Iran Basins: London, The Geological Society, Special Publication 312, 189-203.

Garzanti, E., Critelli, S., Ingersoll, R., 1996, Paleogeographic and paleotectonic evolution of the Himalayan Range as reflected by detrital modes of Tertiary sandstones and modern sands (Indus transect, India and Pakistan): Geological Society of American Bulletin, 108, 631-642.

Garzanti, E., Vezzoli, G., 2003, A classification of metamorphic grains in sandstones based on their composition and grade: Journal of Sedimentary Research, 73, 830-837.

Gazzi, P., 1966, Le arenarie del flysch sopracretaceo dell'Appennino modenese; correlazioni con il flysch di Monghidoro: Mineralogica et Petrographica Acta, 12, 69-97.

Geological Survey of Iran, 1989, Geological map of Iran, scale 1:2500000: Tehran, Iran, Geological Survey of Iran.

Golonka, J., Ford, D., 2000, Pangean (Late Carboniferous-Middle Jurassic) paleoenvironment and lithofacies: Palaeogeography, Palaeoclimatology, Palaeoecology, 161, 1-34.

Gu, X.X., Liu, J.M., Zheng, M.H., Tang, J.X., Qi, L., 2002, Provenance and tectonic setting of the Proterozoic turbidite in Hunan, south China: Geochemistry evidence: Journal of Sedimentary Research, 72, 393-407.

Herron, M.M., 1988, Geochemical classification of terrigeneous sands and shales from core or log data: Journal of Sedimentary Petrology, 58, 820-829.

Ingersoll, R.V., 1978, Petrofacies and petrologic evolution of the Late Cretaceous fore-arc basin, northern and central California: Journal of Geology, 86, 335-352.

Ingersoll, R.V., Suczek, C.A., 1979, Petrology and provenance of Neogene sand from Nicobar and Bengal fans. DSDP sites 211 and 218: Journal of Sedimentary Petrology 49, 1217-1228.

Ingersoll, R.V., Bulard, T.F., Ford, R.L., Grimn, J.P., Pickle, J.P., Sares, S.W., 1984, The effect of grain size on detrital modes: a text of the Gazzi-Dickinson Point Counting method: Journal of Sedimentary Petrology, 54, 103-116.

Jafarzadeh, M., Hosseini-Barzi, M., 2008, Petrography and geochemistry of Ahwaz sandstone member of Asmari formation, Zagros, Iran: Implications of provenance and tectonic setting: Revista Mexicana de Ciencias Geológicas, 25, 247-260.

Javanshir, A.R., Rastad, E., Rabani A.R., 2009, Ore-bearing facies of Ahmad-Abad Zn- Pb (Mo) deposit, northeast of Bafq and comparison with Bleiberg at Alps: Geosciences, 18 (71), 69-80.

Johnson, D.L., 1993, Dynamic denudation evolution of tropical, subtropical and temperate landscapes with three-tiered soils: toward a general theory of landscape evolution: Quaternary International, 17, 67-78.

Joo, J.Y., Lee, I.L., Bai, Z., 2005, Provenance of the Qingshuijian Formation (Late Carboniferous), NE China: Implication for tectonic processes in the northern margin of the North China block: Sedimentary Geology, 177, 97-114.

Krynine, P.D., 1940, Petrology and geneses of the third Bradford Sand: Pennsylvania State College, Mineral Industries Experiment Station Bulletin, 29, 134 pp.

Kutterolf, S., Diener, R., Schacht., U., Krawinkel., H., 2008, Provenance of the Carboniferous Hochwipfel Formation (Karawanken Mountains, Austria/Slovenia)- Geochemistry versus petrography: Sedimentary Geology, 203, 246-266.

Lee, Y.I., 2002, Provenance derived from the geochemistry of late Paleozoic-early Mesozoic mudrocks of the Pyeongan Supergroup, Korea: Sedimentary Geology, 149, 219-235.

Lee, Y.I., 2009, Geochemistry of shales of the Upper Cretaceous Hayang Group, SE Korea: Implications for provenance and source weathering at an active continental margin: Sedimentary Geology, 215, 1-12.

Lee, Y.I., Sheen, D.H., 1998, Detrital modes of the Pyeongan Supergroup (Late Carboniferous-Early Triassic) sandstones in the Samcheog coalfield, Korea: implications for provenance and tectonic setting: Sedimentary Geology, 119, 219-238.

Lev, S.M., Filer, J.K., Tomascak, P., 2008, Orogenesis vs. Diagenesis: Can we use organic-rich shales to interpret the tectonic evolution of a depositional basin: Earth-Science Reviews, 86, 1-14.

González-López, J.M., Bauluz, B., Fernandez-Nieto C., Oliete, A.Y., 2005, Factors controlling the trace-element distribution in fine-grained rocks: the Albian kaolinite-rich deposits of the Oliete Basin (NE Spain): Chemical Geology, 214, 1-19.

Mehring, J.L., McBride, E.F., 2007, Origin of modern quartzarenite beach sands in a temperate climate, Florida and Alabama, USA: Sedimentary Geology, 201, 432-445.

McLennan, S.M., Hemming, S., McDaniel, D.K., Hanson, G.N., 1993, Geochemical approaches to sedimentation, provenance, and tectonics, *in* Johnson, M.J., Basu, A. (eds.), Processes Controlling the Composition of Clastic Sediments: Geological Society of America, Special Paper, 284, 21-40.

McLennan, S.M., Simonetti, A., Goldstein, S.L., 2000, Nd and Pb isotopic evidence for provenance and post-depositional alteration of the Paleoproterozoic Huronian Supergroup, Canada: Precambrian Research, 102, 263-278.

Murali, A.V., Parthasarathy, R., Mahadevan, T.M., Sankar Das, M., 1983, Trace element characteristics, REE patterns and partition coefficients of zircons from different geological environments - a case study on Indian zircons: Geochimica et Cosmochimica Acta, 47, 2047-2052.

Nagarajan, R., Madhavaraju, J., Nagendra, R., Armstrong-Altrin, J.S., Moutte, J., 2007, Geochemistry of Neoproterozoic shales of the Rabanpalli Formation, Bhima Basin, northern Karnataka, southern India: implications for provenance and paleoredox conditions: Revista Mexicana de Ciencias Geologicas, 24(2), 150-160.

Nesbitt, H.W., Young, G.M., 1982, Early Proterozoic climate and plate motions inferred from major element chemistry of lutites: Nature, 299, 715-717.

Nesbitt, H.W., Young, G.M., 1984, Prediction of some weathering trends of plutonic and volcanic rocks based on thermodynamic and kinetic considerations: Journal of Geology, 48, 1523-1534.

Ohta, T., 2004, Geochemistry of Jurassic to earliest Cretaceous deposits in the Nagato Basin, SW Japan: implication of factor analysis to sorting effects and provenance signatures: Sedimentary Geology, 171, 159-180.

Osae, H., Asiedu, D.L., Banoeng-Yakubo, B., Koeberl, C., Dampare, S.B., 2006, Provenance and tectonic setting of Late Proterozoic Beuem sandstones of southeastern Ghana: Evidence from geochemistry and detrital mode: Journal of African Earth Sciences, 44, 85-96.

Passchier, C.W., Trouw, R.A.J., 2005, Microtectonics: Berlin-Heidelberg, Springer-Verlag, 366 pp.

Pettijohn, F.J., Potter, P.E., Siever, R., 1987, Sand and sandstone: New York, Springer-Verlag, 553 pp.

Pirrie D, 1991, Controls on the petrographic evolution of an active margin sedimentary sequence: the Larsen Basin, Antarctica, *in* Morton, A.C., Todd, S.P., Haughton, P.D.W. (eds.), Developments in sedimentary provenance studies: London, The Geological Society, Special Publication 57, 1-11.

Potter, P.E., Maynard, J.B., Pryor, W.A., 1980, Sedimentology of Shale: Berlin, Springer-Verlag, 400 pp.

Roser, B.P., Korsch, R.J., 1988, Provenance signature of sandstone-mudstone suite determined using discriminant function analysis of major element data: Chemical Geology, 67, 119-139.

Saeedi, M., Hosseini-Barzi, M., 2010, Petrology and major element geochemistry of the Devonian Padeha Formation: Implications for provenance, geotectonic setting and paleoclimate conditions, *in* Actas Inageq, 16, 330-332.

Seyed-Emami, K., 2003, Triassic in Iran: Facies, 48, 95-106.

Shadan, M., Hosseini-Barzi, M., 2009, Geochemistry of Khan Formation

sandstones in central Iran: implications for provenance studies, *in* 27th IAS Meeting of Sedimentology, Alghe: Italy, p. 349.

Stampfli, G.M., Borel, G.D., 2002, A plate tectonic model for the Paleozoic and Mesozoic constrained by dynamic plate boundaries and restored synthetic oceanic isochrones: Earth and Planetary Science Letters, 196, 17-33.

Suttner, L.J., Dutta, P.K., 1986, Alluvial sandstone composition and paleoclimate, I. Framework mineralogy: Journal of Sedimentary Geology, 56, 329-345.

Suttner, L.J., Basu, A., Mack, G.M., 1981, Climate and the origin of quartz arenites: Journal of Sedimentary Petrology, 51, 1235-1246.

Taylor, S.R., McLennan, S.M., 1985, The Continental Crust: its Composition and Evolution: Oxford, Blackwell, 312 pp.

van de Kamp, P.C., Leake, B.E., 1995, Petrology and geochemistry of siliciclastic rocks of mixed feldspathic and ophiolitic provenance in the Northern Apennines, Italy: Chemical Geology, 122, 1-20.

van Hattum, M.W.A., Hall, R., Pickard, A.L., Nichols, G.J., 2006, Southeast Asian sediments not from Asia: Provenance and geochronology of north Borneo sandstones: Geology, 34, 589-592.

Verma, S.P., 1997, Sixteen statistical tests for outlier detection and rejection in evaluation of international geochemical reference material: Example of microgabbro PM-S: Geostandards Newsletter, 21, 59-75.

Verma, S.P., 2005, Estadística Básica para el Manejo de Datos Experimentales: Aplicación en la geoquímica (geoquimiometría): México, D.F., Universidad Nacional Autónoma de México, 186 pp.

Verma, S.P., 2009, Evaluation of polynomial regression models for the Student t and Fisher F critical values, the best interpolation equations from double and triple natural logarithm transformation of degrees of freedom up to 1000, and their applications to quality control in science and engineering: Revista Mexicana de Ciencias Geológicas, 26, 79-92.

Verma, S.P., 2012, Geochemometrics: Revista Mexicana de Ciencias Geológicas, 29, 276-298.

Verma, S.P., Díaz-González, L., 2012, Application of the discordant outlier detection and separation system in the geosciences: International Geology Review, 54, 593-614.

Verma, S.P., Quiroz-Ruiz, A., 2008, Critical values for 33 discordancy test variants for outliers in normal samples for very large sizes of 1,000 to 30,000: Revista Mexicana de Ciencias Geológicas, 25, 369-381.

Verma, S.P., Quiroz-Ruiz, A., 2011, Corrigendum to Critical values for 22 discordancy test variants for outliers in normal samples up to sizes 100, and applications in science and engineering [Rev. Mex. Cienc. Geol., 23 (2006), 302-319]: Revista Mexicana de Ciencias Geológicas, 28, 202.

Verma, S.P., Santoyo, S., 2005, Is odd-even effect reflected in detection limits?: Accreditation and Quality Assurance, 10, 144-148.

Verma, S.P., Santoyo, E., Velasco-Tapia, F., 2002, Statistical evaluation of analytical methods for the determination or rare-earth elements in geological materials and implications for detection limits: International Geology Review, 44, 287-335.

Verma, S.P., Quiroz-Ruiz, A., Díaz-González, L., 2008, Critical values for 33 discordancy test variants for outliers in normal samples up to sizes 1000, and applications in quality control in Earth Sciences: Revista Mexicana de Ciencias Geológicas, 25, 82-96.

Verma, S.P., Díaz-González, L., González-Ramírez, R., 2009, Relative efficiency of single outlier discordancy tests for processing geochemical data on reference materials and application to instrumental calibrations by a weighted least-squares linear regression model: Geostandards and Geoanalytical Research, 33, 29-49.

Weaver, C.E., 1989, Clays, Muds and Shales: Amsterdam, Elsevier, 818 pp.

Wei, G.J., Liu, Y., Li, X.H., Shao, L., Fang D., 2004, Major and trace element variations of the sediments at ODPSite 1144, South China Sea, during the last 230 ka and their paleoclimate implications: Palaeogeography, Palaeoclimatology, Palaeoecology, 212, 331-342.

Wilmsen, M., Fursich, F.T., Seyed-Emami, K., Majidifard, M.R., 2009, An overview of the stratigraphy and facies development of the Jurassic System on the Tabas Block, east-central Iran, *in* Brunet, M F., Wilmsen, M., Granath, J.W., (eds.), South Caspian to Central Iran Basins: London, The Geological Society, Special Publication 312, 323-343.

Wronkiewicz, D.J., Condie, K.C., 1989, Geochemistry and provenance of sediments from the Pongola Supergroup, South Africa: evidence for a 3.0-Ga-old continental craton: Geochimica et Cosmochimica Acta, 53, 1537-1549.

Zanchi, A., Zanchetta, A, S. Berra, F., Mattei, M., Garzanti, E., Molyneux, S., Nawab, A., Sabouri, J., 2009, The Eo-Cimmerian (Late? Triassic) orogeny in North Iran, *in* Brunet, M F., Wilmsen, M., Granath, J.W., (eds.), South Caspian to Central Iran Basins: London, The Geological Society, Special Publication 312, 31-55.

Manuscript received: January 17, 2012
Corrected manuscript accepted: September 4, 2012
Manuscript accepted: October 15, 2012